Electromagnetic Performance Optimization for Five-phase Bearingless PMSM with Third Harmonic Injection

Yuemei Qin, Huangqiu Zhu, Yizhou Hua

School of Electrical and Information Engineering, Jiangsu University, Zhenjiang 212013, Jiangsu, China

25th International Conference on Magnet Technology

Paper ID: Mon-Af-Po1.05-11 [80]

Background

For the virtues of non-friction, high-speed and long life, etc., bearingless motors have wide application prospects in high-purity and high-speed areas. As a five-phase motor, the torque density can be further increased when the third-order harmonic current is injected. However, the rotor MMF produced by square-shape surface-mounted permanent magnets (SMPMs) contains abundant harmonic resulting in large torque ripple. Although the torque ripple can be decreased by optimizing the SMPMs into sine-shape, it has adverse effect on output torque. To balance the contradiction mentioned above, a five-phase 10-slot/8-pole bearingless PMSM (10/8 BPMSM) is proposed in this paper.

Electromagnetic Performance Optimization for Five-phase Bearingless PMSM with Third Harmonic Injection

Objectives

- The torque and suspension force of the saddle shaping PM motor is improved by 13% and 6.8% when compared with sine shaping PM motor.
- The torque and suspension force ripple are reduced by 16.1% and 6.7% when compared with square shaping PM motor.

Conclusion

- The mathematical model of stator magnetic motive force is first established in detail based on the winding function method.
- The permanent magnet (PM) is optimized to saddle shaping which only contains the fundamental and 3rd harmonic.
- The principle of suspension force is elaborated based on the harmonics interaction between stator and rotor MMF, and the influence of interaction between high harmonics on the main suspension force is analyzed in detail.
- The PM with sine and square shaping are designed, and the electromagnetic performance including the cogging torque, the torque and suspension force and their ripple are compared and analyzed.
- The motor with the saddle shaping and sine shaping PM are prototyped and experimented to validate the analyses.

Methods

The MMF of Stator and Rotor

$$f_s = n_{sj}(\theta)\times i_{sj}(t) =$$

$$\sum_{j=1}^{10}\sum_{v}^{\infty}\sum_{m}^{\infty} n_{2v} I_{sm} \cos v[\theta-\frac{2\pi}{j}(j-1)]\times\cos m[\omega t-\frac{2\pi}{j}P_B(j-1)]$$

$$=\begin{cases}5F_B\cos(m\omega t+v\theta), & v+mP_B=10k(k=0,1,2,\ldots)\\ 0, & v\pm mP_B\neq 10k(k=0,1,2,\ldots)\\ 5F_B\cos(m\omega t-v\theta), & v-mP_B=10k(k=0,1,2,\ldots)\end{cases}$$

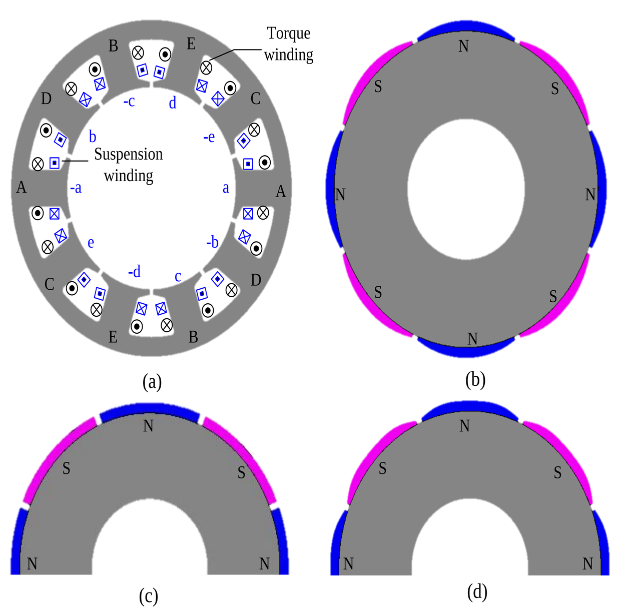

The stator MMF produced by the mth suspension force current has $10k \pm mP_B$ harmonic such as 3rd, 7th, 13th … generated by suspension force fundamental current, where k is an integer making v be positive integer. Similarly, the stator MMF produced by the mth torque current has $10k \pm mP_M$ harmonic such as 4th, 6th, 14th … and 2nd, 8th, 12th … generated by the fundamental and third-order harmonic torque current, respectively

Interaction of air gap MMF between stator and rotor

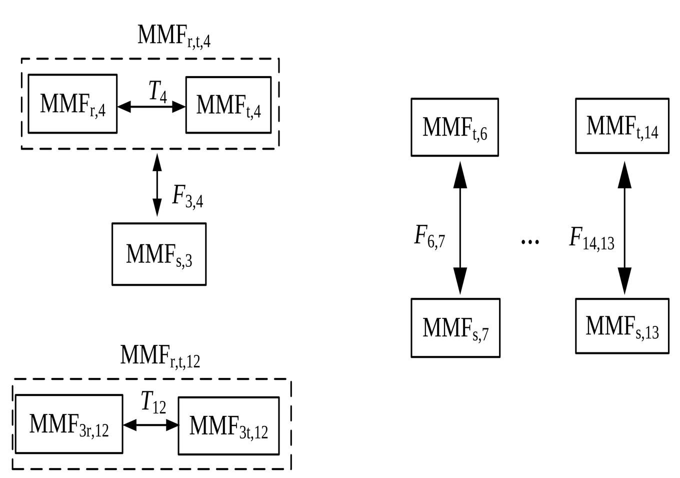

- The synthesis air-gap MMF$_{r,t,4}$ generated by the 4th rotor and stator MMF interacts with the 3rd stator MMF$_{s,3}$ to produce a constant suspension force $F_{3,4}$.
- The amplitude of the 6th stator MMF is only 1.5% of the MMF$_{r,t,4}$, so the suspension force $F_{6,7}$ and $F_{13,14}$ etc. can be negligible.
- The MMF$_{3r,12}$ interacts with the MMF$_{3t,12}$ to enhance the torque.

The Mathematical Model of the Suspension Force

$$\begin{cases}F_x = h_m I_{Mf} I_s \cos(\varphi_{Mf}-\varphi_B)\\ F_y = h_m I_{Mf} I_s \sin(\varphi_{Mf}-\varphi_B)\end{cases}$$

The magnitude of the suspension force is proportional to the suspension force current I_s, while the direction is determined by the difference between φ_{Mf} and φ_B.

$$h_m = 25\sin\frac{\pi}{10}\sin\frac{2\pi}{10}\frac{\mu_0 lrN_1N_2k_1k_2}{\pi\delta_0^2}$$

Samples

Structure diagram of the motor

parameters	FSCDW BPMSM
Inner/outer diameter of the stator	102/168 mm
Inner/outer diameter of the rotor	42/94 mm
Permanent magnets thickness	3 mm
Air gap thickness	1 mm
Turn number of the torque/suspension force windings	20/50
Amplitude of the torque/suspension force current	5/5A

Results

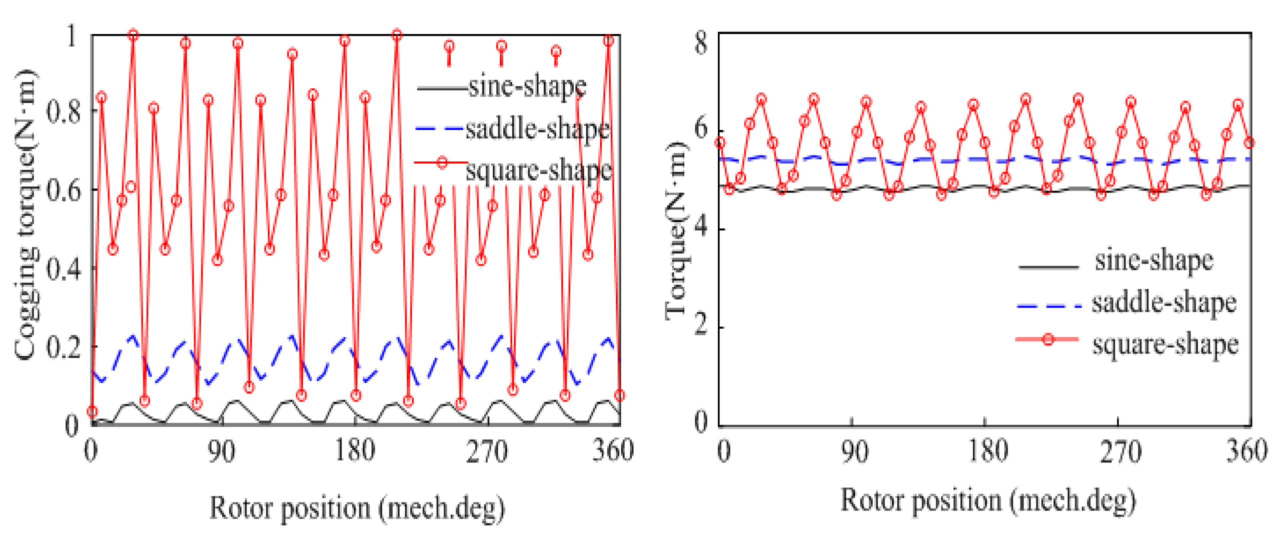

The torque of the saddle shaping PM motor is improved by 13% when compared with sine shaping PM motor. While and the torque and suspension force ripple are reduced by 16.1% when compared with square shaping PM motor.

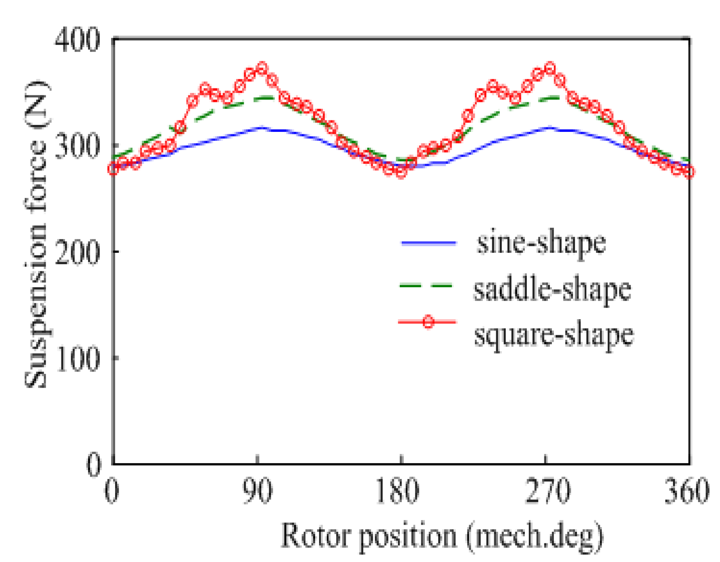

The suspension force of the saddle shaping PM motor is improved by 6% when compared with sine shaping PM motor. While and the suspension force ripple are reduced by 6.7% when compared with square shaping PM motor.

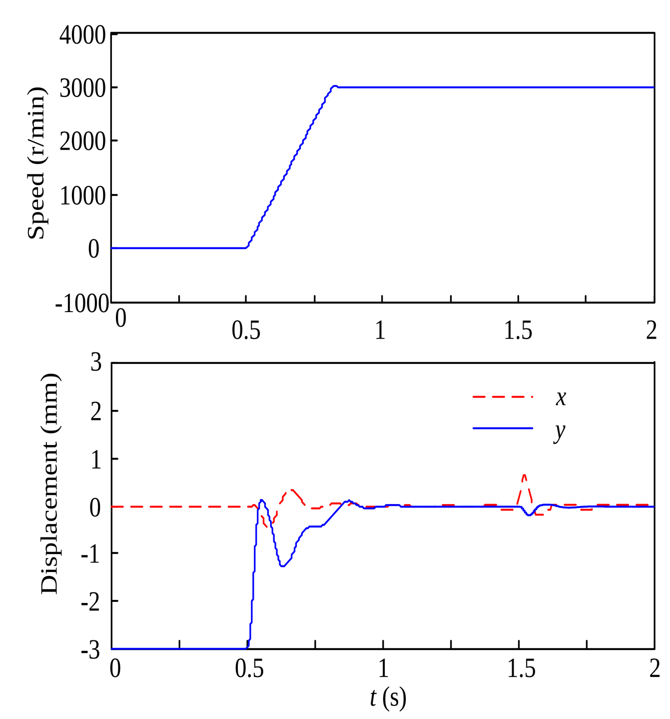

When the speed reference steps from 0 to 3 000 r/min at t = 0.5 s, there are about 40 and 120 μm fluctuations of the radial displacements in x- and y-directions, respectively. After 1.5 s, a 20 N radial disturbance is imposed on the suspended rotor in the x-axis, and the deviation values of radial displacements in x- and y-axis are 80 μm and 20 μm respectively.

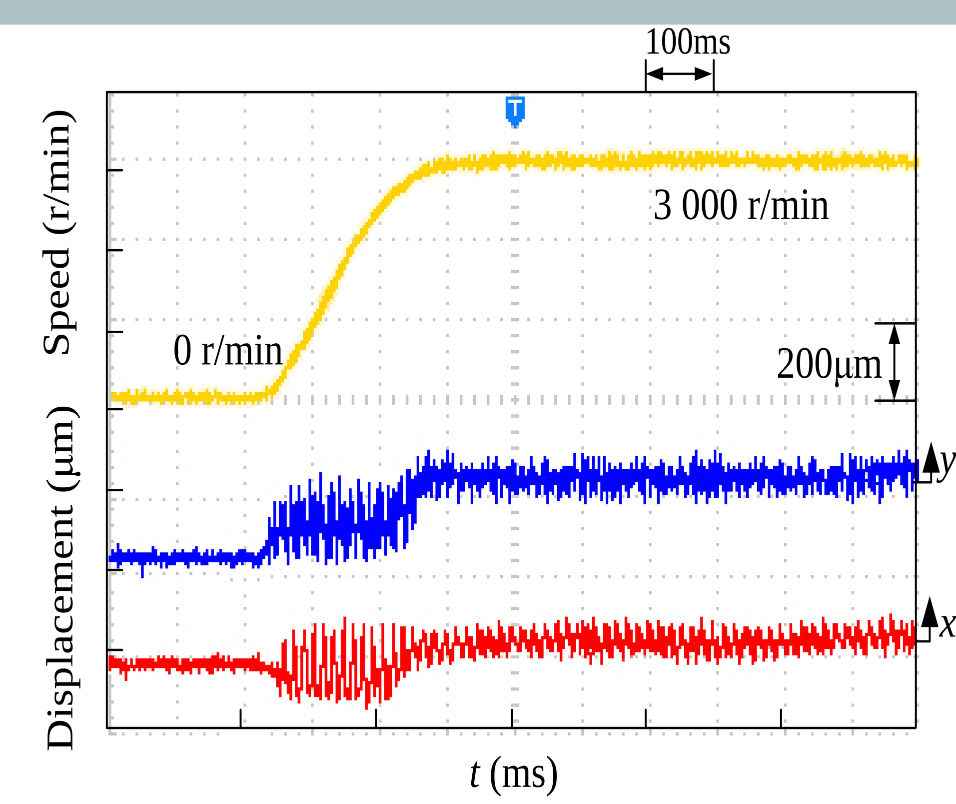

When the dynamic rotation speed waveforms of the prototype which changes from 0 r/min to 3 000 r/min, the measured speed can track the speed command quickly. Meanwhile, disturbance of the rotor radial displacements in the x- and y-axis direction are smaller than 0.3 mm when the rotor speed is from 0 to 3 000 rpm.